Exposure to the gut microbiota from cigarette smoke-exposed mice exacerbates cigarette smoke extract-induced inflammation in zebrafish larvae

Simone Morris[1]†, Kathryn Wright[1], Vamshikrishna Malyla[2,3], Warwick J Britton[1,4], Philip M Hansbro[2], Pradeep Manuneedhi Cholan[1] *†, Stefan H Oehlers[1,5] *

Affiliations
1 Tuberculosis Research Program at the Centenary Institute, The University of Sydney, Camperdown, NSW, Australia.
2 Centre for Inflammation, Centenary Institute and University of Technology Sydney, Faculty of Science, School of Life Sciences, Sydney, NSW, Australia.
3 Discipline of Pharmacy, Graduate School of Health, University of Technology Sydney, Sydney, NSW, Australia.
4 Department of Clinical Immunology, Royal Prince Alfred Hospital, Camperdown, Australia.
5 The University of Sydney, Faculty of Medicine and Health, Camperdown, NSW, Australia
† Co-first authors, contributed equally
* Co-corresponding authors: pradeep.manuneedhicholan@mq.edu.au or s.oehlers@centenary.org.au

Abstract
Cigarette smoke (CS)-induced inflammation leads to a range of diseases including chronic obstructive pulmonary disease and cancer. Environmental factors including gut microbiota make up are major modifying factors that determine the severity of cigarette smoke-induced pathology. Adult zebrafish display increased inflammatory cytokine transcription when exposed to cigarette smoke extract (CSE) but incongruously do not produce a mucosal leukocytic inflammation phenotype. Zebrafish embryos and larvae have been used to model the effects of cigarette smoking on a range of physiological processes and offer an amenable platform for screening modifiers of cigarette smoke-induced pathologies. Here we exposed zebrafish larvae to CSE and showed that it was toxic and we characterised a CSE-induced leukocytic inflammatory phenotype with increased neutrophilic and macrophage responses. The CSE-induced phenotype was exacerbated by co-exposure to microbiota from the faeces of CS-exposed mice, but not control mice. Microbiota could be recovered from the gut of zebrafish and studied in isolation. This demonstrates the utility of the zebrafish-CSE exposure platform for identifying environmental modifiers of cigarette smoking-associated pathology and demonstrates that the CS-exposed mouse gut microbiota potentiates the inflammatory effects of CSE across host species.

Introduction

Smoking tobacco is one of the greatest public health challenges, accounting for more than 8 million deaths worldwide, per year (1). It ranks as the third leading risk factor for illness and death, including from diseases such as cancers and inflammatory disorders like inflammatory bowel disease (IBD) (1-4). Cigarette smoke (CS) contains a multitude of toxic compounds affecting cell function, foetal development, gut function and microbiome, neural activity, inflammation, and lung cancer (3, 5-12).

The toxicity of CS has further been demonstrated to alter the microbiome of smokers, resulting in respiratory and gut microbiome dysbiosis, which in turn is associated with increased peptic ulcers, IBD and gastrointestinal cancers via the gut-lung axis of shared mucosal immunity (3, 4, 6, 11, 13). This is suggested to occur through alterations to the immune system (5), mucin production (6) or through direct anti-microbial effects of the toxins within the smoke (14). Shifts in gut microbiome and the profile of gut metabolites and pathology are associated with COPD in humans and CS-induced emphysema in mice (4, 10, 11, 15, 16). COPD- and CS-associated microbiomes and metabolites exacerbate lung inflammation via the gut-lung axis of shared mucosal immunity contributing to lung pathology (4, 11, 17).

Zebrafish have been used to study the developmental defects caused by CS exposure. These studies demonstrated stunted embryonic development upon exposure to CSE and smoke condensate (18-20). CSE exposure of adult zebrafish reduced the capacity for fin regeneration (19), as well as behavioural abnormalities in response to nicotine (7). A study by Progatzky *et al.* further modelled the respiratory effects of CS using adult zebrafish gills demonstrating increased pro-inflammatory cytokine production and reduced immune cell recruitment (21). Massarsky *et al.* used total particulate matter (TPM) from cigarettes to model the effects of CS in zebrafish, and showed cardiac malfunction and defects in brain vascularisation (22) as well as behavioural alterations (23).

Thus far, the effect of CS exposure on immune function has been unexplored in zebrafish embryos and larvae (19, 21). This transparent stage of development provides the opportunity to investigate the inflammatory effects of CSE by live imaging of fluorescently tagged leukocytes, and is amenable to simplified experimental manipulation by gene editing or treatment with small molecules by immersion (24). Here we define the pro-inflammatory effects of CSE on larval zebrafish and find a transferrable effect of mammalian CS-associated microbiota on CSE-induced inflammation in larval zebrafish.

Methods

Zebrafish husbandry

Zebrafish embryos were obtained through natural spawning (Sydney Local Health District Animal Welfare Committee Approval 17-036). The transgenic strains used to visualise leukocytes were *Tg(lyzC:DsRed)*^{nz50}, where neutrophils are labelled by DsRed2 expression (25), and *Tg(mfap4:turquoise)*^{xt27}, where macrophages are labelled by Turquoise2 (26). Embryos were raised in E3 media supplemented with methylene blue in a dark incubator at 28°C until 1 day post fertilisation (dpf). Cleaned 1 dpf embryos were transferred to E3 without methylene blue and reared (dark incubator, 28°C) until used.

Preparation of CS

CSE was prepared by using a custom-built smoking device where reference cigarette 3R4F (Kentucky Tobacco Research & Development Centre) was lit using a lighter and CS was bubbled directly in to 10 mL of PBS until the whole cigarette was exhausted. This 10 mL of CSE was filtered using a 0.22-micron filter to remove CS-derived debris. This preparation of the smoke of one cigarette per 10 mL PBS is considered 100% CSE and was diluted as indicated. CSE was prepared fresh before treatment.

CSE exposure

Embryos/larvae were exposed to CSE at a density of approximately 1 larva per mL of E3 in plastic Petri dishes at the ages indicated, either 3 or 5 dpf, and maintained in a dark incubator at 28°C. The stock solution of 100% CSE in PBS was diluted directly into E3 zebrafish media. Filter sterilised PBS was used as vehicle control.

90 Zebrafish behavioural analysis
91 Zebrafish larvae were transferred to a 24-well plate with 1 embryo per well in their CSE-supplemented E3
92 media. The plate was transferred to a ZebraBox (Viewpoint) and locomotion was recorded for 15 minutes.
93 Video files were analysed using EthoVision XT 11 (Noldus) using the following parameters: sensitivity 110,
94 video pixel smoothing low, subject size 4-4065. Locomotion analysis was calculated as the total distance
95 travelled (mm) of individual larva over the recording window.
96
97 Tail transection assays
98 Caudal fin amputations were performed on 5 dpf larvae. Larvae were anesthetised with 2.5% (v/v) ethyl-3-
99 aminobenzoate methanesulfonate (tricaine) (Sigma, E10521), wounded posterior to the notochord using a
100 sterile scalpel and kept in a 28°C incubator to recover as previously described (27). Wounded larvae were
101 imaged at 6 hours post wounding.
102
103 Imaging and image analysis
104 Larvae were imaged using a Leica M205FA fluorescent microscope. ImageJ software was used to quantify
105 fluorescent pixel counts as previously described (27).
106
107 Generation of microbiome-depleted zebrafish embryos
108 Microbiome-depleted zebrafish were created and maintained as previously described (28). Briefly, freshly
109 laid embryos were rinsed with 0.003% v/v bleach in sterile E3 and rinsed 3 times with sterile E3. Bleached
110 embryos were raised in sterile E3 supplemented with 50 µg/mL ampicillin (Sigma), 5 µg/mL kanamycin
111 (Sigma) and 250 ng/mL amphotericin B (Sigma) in sterile tissue culture flasks. Dead embryos and chorions
112 were aseptically removed at 1 and 3 dpf, respectively.
113
114 Generation of mouse faecal microbiota specimens
115 Mice were housed at the Centenary Institute (Sydney Local Health District Animal Welfare Committee
116 Approval 2020-003). C57BL/6J mice were housed in a pathogen-free and temperature-controlled
117 environment, with 12 hours of light and 12 hours of darkness, and free access to food and water. Mice
118 were smoked with 12x 3R4F cigarettes for 75 minutes, twice a day, 5 days per week for 10 weeks by using a
119 custom-designed and purpose-built nose-only, directed flow inhalation and smoke-exposure system (CH
120 Technologies, NJ) (10, 29). This is representative of a pack-a-day smoker (2).
121
122 Faecal pellets were collected from mice that were housed in different cages. Individual faecal pellets were
123 collected into sterile 1.7 mL microcentrifuge tubes and homogenised in 1 mL of sterile E3 by pipetting.
124 Homogenised specimens were centrifuged (500 x*g*, 2 minutes) to sediment fibrous material and
125 supernatant were collected then pooled. Pooled supernatants were supplemented with glycerol to a final
126 concentration of 25% v/v, aliquoted, and frozen at -80°C before use.
127
128 Exposure of zebrafish larvae to mouse faecal microbiota
129 Microbiome-depleted zebrafish were rinsed at 3 dpf with sterile E3, without antibiotic and amphotericin B
130 supplementation, and colonised by the addition of 200 µL thawed faecal homogenate supernatant into 30
131 mL sterile E3 delivering a final concentration of ~$5x10^4$ CFU per mL. Enumeration of culturable bacterial
132 load was carried out by culture under aerobic conditions at 28°C on LB agar (Thermofisher).
133
134 Detection of gene expression
135 Groups of at least 10 larvae were homogenised in Trizol (Thermofisher) and processed for RNA extraction
136 as per manufacturer's instructions. cDNA was reverse transcribed using the Applied Biosystems High
137 Capacity cDNA synthesis kit (Thermofisher) from 2 µg of total RNA. Quantitative PCR was carried out on a
138 CFX Connect machine (Biorad) with Powerup SYBR reagent (Thermofisher), primer sets were (5'-3'): *il1b* Fw
139 ATCAAACCCCAATCCACAGAGT, Rv GGCACTGAAGACACCACGTT; *18s* Fw TCGCTAGTTGGCATCGTTTATG, Rv
140 CGGAGGTTCGAAGACGATCA.
141
142 Statistical analysis

143 Statistical testing was carried out by ANOVA with post hoc multiple comparisons as appropriate using
144 GraphPad Prism. Data are expressed as mean ± SD. Outliers were excluded using a 1% ROUT test. Every
145 datapoint represents a single embryo unless otherwise noted as for qPCR analyses.
146
147 **Results**
148 CSE is toxic to zebrafish larvae
149 To establish a survivable dose of CSE that did not cause gross pathology, we exposed 3 dpf zebrafish larvae
150 to a range of CSE doses and monitored survival. We found exposure at up to 2% CSE was tolerated by
151 zebrafish larvae (Figure 1A), with no overt changes to morphology (Figure 1B). Exposure to 3% CSE caused
152 significant mortality within 1 day post exposure.
153
154 To verify that the CSE was bioactive at 1% and 2% concentrations, we tracked larval motility to detect
155 nicotine-induced increases in motility at 5 dpf, or 2 days post exposure (30). Exposure to 1% or 2% CSE
156 increased the total distance travelled of zebrafish larvae compared to mock exposed larvae in a 15 minute
157 recording period indicating components of the CSE were still bioactive after 2 days of immersion exposure
158 in E3 media (Figure 1C).
159
160 We next used *Tg(lyzC:DsRed)*^{nz50} larvae to visualise neutrophils and *Tg(mfap4:turquoise)*^{xt27} to visualise
161 macrophages (25, 26). Immune cell fluorescent area was used as a proxy to estimate changes to immune
162 cell number by non-invasive live imaging. We performed tail transection on 5 dpf larvae that had been
163 exposed to CSE from 3 dpf and assessed leukocyte recruitment to the wound at 6 hours post wounding.
164 While neutrophil recruitment was slightly but statistically significantly reduced by 1% CSE, there was no
165 effect of 2% CSE exposure compared to vehicle control and overlap between neutrophil recruitment in the
166 1% and 2% CSE exposure groups (Figure 1D). There was significantly more macrophage recruitment to
167 wounds in 2% CSE-exposed larvae compared to control and 1% CSE larvae (Figure 1E).
168
169 Acute exposure to CSE induces myelopoiesis in zebrafish larvae
170 To examine the acute effects of CSE exposure on larvae after major organogenesis is complete, we exposed
171 5 dpf larvae to CSE for 24 hours. Immersion in 1% and 2% CSE caused a gradated increase in total
172 neutrophil fluorescent area in zebrafish larvae compared to PBS vehicle (Figure 2A and 2B). This
173 inflammatory effect of CSE appeared stronger on total macrophage fluorescent area with a statistically
174 significant increase in total macrophages in 2% CSE-exposed compared to control larvae (Figure 2C and 2D).
175
176 Acute exposure to CSE induces an inflammatory response in the gut of zebrafish larvae
177 The effects that we observed suggested that CSE induced inflammatory haematopoietic response. Since the
178 larval midgut and hindgut is an important site of immune response to chemical irritants, we next quantified
179 leukocyte recruitment to the larval intestine (31). Leukocyte fluorescence was increased in the gut of 6 dpf
180 larvae that had been exposed to 2% CSE from 5 dpf compared to either control or 1% CSE-exposed larvae
181 (Figure 3A and 3B). However, the estimation of gut macrophages by fluorescent pixel count in our
182 *Tg(mfap4:turquoise)*^{xt27} larvae was potentially confounded by luminal autofluorescence that was more
183 noticeable in CSE-exposed larvae (Figure 2B).
184
185 The enhanced effects of CSE on innate immune cell numbers in the larval gut led us to hypothesise that the
186 microbiota may interact with CSE to drive inflammation at zebrafish larval mucosal surfaces as observed
187 with other chemical irritants (31, 32). Thus, we next examined the effect of CSE and the role of changes in
188 the endogenous microbiota by depleting bacteria with broad spectrum antibiotics prior to CSE exposure
189 from 5 to 6 dpf. Antibiotic treatment did not affect the ability of 2% CSE to increase neutrophil or
190 macrophage fluorescence in the larval gut suggesting that gut microbiota are not necessary to drive the
191 acute inflammatory effects of 2% CSE (Figure 3A and 3B).
192
193 CS-exposed mouse microbiota increases the neutrophilic inflammatory effects of CSE
194 We next assessed if the microbiota of chronically CS-exposed mice could impart increases in sensitivity to
195 CSE exposure by exposing 3 dpf microbiota-depleted larval zebrafish to faecal homogenate from mice
196 exposed to CS/air controls for 10 weeks and CSE. We used the suboptimal concentration of 1% CSE, which

did not induce intestinal inflammation in our acute exposure assay, to detect enhancement of inflammation by microbiota derived from the faeces of CS-exposed mice.

The total count of neutrophil fluorescence was unaffected in 5 dpf larvae immersed with microbiota from CS- or normal air-exposed control mice, and the addition of 1% CSE (Figure 4A and 4B).

Exposure to microbiota from CS-exposed or control mice did not affect neutrophil fluorescence in the gut of wild-type 5 dpf larvae compared to germ-free reared larvae (Figure 4C and 4D). Addition of 1% CSE did not affect neutrophil fluorescence in the gut in 5 dpf larvae raised microbiota-depleted or in those exposed to microbiota from control non-smoked mice. However, 5 dpf larvae that had been exposed to microbiota from smoked mice and 1% CSE had significantly more neutrophil fluorescence in the gut than any of the control groups. This pattern was replicated by *il1b* transcription levels quantified by RT-qPCR (Figure 4E).

<u>CS-exposed mouse microbiota increases the macrophage inflammatory effects of CSE</u>

Analysis of *Tg(mfap4:turquoise)*^{xt27} macrophage reporter larvae revealed increased total macrophage fluorescence in 5 dpf larvae that that had been exposed to microbiota from CS-exposed mice and 1% CSE compared to any of the control groups, except for the air-exposed mouse microbiota and 1% CSE control group (Figure 5A and 5B). Quantification of gut macrophage fluorescence was again confounded by luminal autofluorescence in CSE-exposed larvae, appearing to be elevated in all CSE-exposed groups (Figure 5C and 5D).

CS-exposed faecal microbiota contains culturable bacteria that do not affect inflammatory responses

To investigate if any individual species of bacteria from CS-exposed mouse microbiota were able to recapitulate the effects of exposure to the bulk microbiota homogenate, we recovered bacteria from the homogenised CS-exposed mouse microbiota-exposed larvae onto rich LB agar. Four species were subcultured to purity by passage on LB agar and genotyped by 16s sequencing as *Acinetobacter radioresistens*, *Bacteroides vulgatus*, *Enterobacter cancerogenus*, and *Stenotrophomonas maltophilia* (Supplementary File). We then screened these individual bacteria by colonising 3 dpf microbiota-depleted larvae in combination with 1% CSE exposure and found no effect on total or gut leukocyte fluorescent area (Figure 6).

Discussion

Here we found the immune system of zebrafish larvae is sensitive to the pro-inflammatory neutrophilic and macrophage effects of CSE. Exposing zebrafish larvae to microbiota derived from the faeces of CS-exposed mice demonstrate the presence of microbes (including culturable *Acinetobacter radioresistens*, *Bacteroides vulgatus*, *Enterobacter cancerogenus*, and *Stenotrophomonas maltophilia*) or metabolites capable of amplifying the inflammatory effects of CSE across species. Together, these data establish zebrafish larvae as a platform for studying the environmental interactions that affect cigarette- and tobacco-induced inflammatory damage.

Our finding that CSE concentrations of >2% are toxic to zebrafish larvae are in line with previous studies by Alvarez *et al.* who showed larvae can survive in a solution of approximately 1% CSE and Progatzky *et al.* who utilised a 1% CSE challenge with adult zebrafish (19, 21). Exposure of adult zebrafish to CSE by Alvarez *et al.* demonstrated an impairment in post-amputation fin regeneration (19). Our acute wound leukocyte response data adds to this observation by suggesting that increased numbers of wound-associated macrophages may impede physiological regeneration in the presence of CSE.

Our data demonstrate that exposure of zebrafish larvae to 2% CSE causes an expansion of leukocytes (neutrophils and macrophages) and leukocytic inflammation in the gut. Despite the increased leukocyte fluorescent area, we did not observe the mass redistribution of leukocytes to the skin mucosal surfaces as we have previously documented with the enterocolitis-inducing chemical irritants dextran sodium sulfate and 2,4,6-trinitrobenzene sulfonic acid (31, 32). Exposure of zebrafish larvae to a dose of 1% CSE did not cause detectable changes to inflammatory markers in conventionally reared larvae. Our results are comparable to work using adult zebrafish that found only a subtle inflammatory response to 1% CSE

exposure in the gill tissue of adult zebrafish with upregulation of inflammatory gene expression but decreased or unchanged immune cell infiltration in the gills depending on the length of exposure (21).

Our system of using a low dose of 1% CSE for two days to stimulate a below measurable amount of inflammation proved sensitive to modulation by microbiota samples from CS-exposed mouse faeces. Zebrafish have been used to as hosts for trans-species microbiota transplants (33, 34), and our study expands this knowledge by demonstrating sensitivity of recipient zebrafish host inflammation to a microbiota-environment interaction. This proof-of-concept data suggests that zebrafish larvae may be a feasible platform with which human microbiota-CS interactions can be screened to uncover potential missing links in microbiota-environment interactions that appear to predispose some smokers to the development of COPD (4, 9, 11).

The failure of single bacterial species that could be cultured from the guts of zebrafish to recapitulate the pro-inflammatory effects of CS-exposed mouse microbiota in the context of 1% CSE co-exposure suggest either the presence of multiple microbial species and/or other microbiota or factors present in the faecal homogenate. This was not unexpected as the aerobic conditions of the larval zebrafish gut does not facilitate sustained colonisation by some members of the mammalian microbiota (33), and recent mouse studies have demonstrated the importance of the metabolome, including short chain fatty acid output, in susceptibility to smoking-induced pathology (15, 16, 35). Given the lack of butyrate production found in conventionally raised zebrafish larvae (27), we think it is unlikely that exposure to control mouse faecal microbiota produces anti-inflammatory short chain fatty acids as the protective mechanism against 1% CSE exposure compared to the pro-inflammatory CS-exposed mouse faecal microbiota. Instead, we propose that the presence of additional toxins or pro-inflammatory factors either already present or produced by complex mixtures of microbes harvested from the supernatant of faecal homogenates drives inflammatory responses.

The dose response effects of CSE exposure on inflammation in larval zebrafish suggest this platform could be adapted for use as a screening platform to identify positive and negative regulators of inflammation (36). In this study we have demonstrated the utility of a low CSE challenge to identify CS-associated microbiota as factors that increase the susceptibility of zebrafish larvae to CSE-induced inflammation. Follow-up studies would identify other soluble environmental factors that increase the inflammatory potential of CSE. Conversely, a higher dose of 2% CSE challenge could be used as a platform to screen for inhibitors of CSE-induced inflammation. Since we have recently demonstrated the sensitivity of zebrafish larval inflammation to the short chain fatty acid butyrate (27), it would be interesting to determine if high dose CSE-induced inflammation in zebrafish larvae can also be ameliorated by butyrate supplementation.

In summary, we have demonstrated the suitability of zebrafish larvae for studying the inflammatory effects of cigarette smoke-environment interactions and show that the CS-exposed mouse gut microbiota potentiates the inflammatory effects of CSE across host species.

DATA AVAILABILITY

Raw data is available upon reasonable request to the corresponding authors.

ACKNOWLEDGEMENTS

We thank other members of the Oehlers lab at the Centenary Institute for their input into this work and maintenance of the zebrafish aquarium; Dr Angela Fontaine and Sydney Cytometry for assistance with imaging; Dr Diana Quan and Ms Trixie Wang for collection of mouse faeces; Dr Kamal Dua for supervision of VM.

FUNDING

This work was supported by a Centenary Institute Summer Scholarship to S.M.; University of Sydney Fellowship [grant number G197581] and NSW Ministry of Health under the NSW Health Early-Mid Career Fellowships Scheme [grant number H18/31086] to S.H.O.; the NHMRC Centre of Research Excellence in Tuberculosis Control (APP1153493) to W.J.B.; NHMRC Fellowship (APP1175134) UTS, Cancer Council NSW

(1157073), and the Rainbow Foundation to P.M.H.; Graduate School of Health and University of Technology Sydney (UTS President's scholarship and UTS International Research Scholarship) to V.M..

References

1. WHO. Tobacco 2021 [Available from: https://www.who.int/news-room/fact-sheets/detail/tobacco.
2. Jones B, Donovan C, Liu G, Gomez HM, Chimankar V, Harrison CL, et al. Animal models of COPD: What do they tell us? Respirology. 2017;22(1):21-32.
3. Keely S, Talley NJ, Hansbro PM. Pulmonary-intestinal cross-talk in mucosal inflammatory disease. Mucosal Immunol. 2012;5(1):7-18.
4. Budden KF, Gellatly SL, Wood DL, Cooper MA, Morrison M, Hugenholtz P, et al. Emerging pathogenic links between microbiota and the gut-lung axis. Nat Rev Microbiol. 2017;15(1):55-63.
5. Verschuere S, Bracke KR, Demoor T, Plantinga M, Verbrugghe P, Ferdinande L, et al. Cigarette smoking alters epithelial apoptosis and immune composition in murine GALT. Laboratory Investigation. 2011;91(7):1056-67.
6. Allais L, Kerckhof FM, Verschuere S, Bracke KR, De Smet R, Laukens D, et al. Chronic cigarette smoke exposure induces microbial and inflammatory shifts and mucin changes in the murine gut. Environmental microbiology. 2016;18(5):1352-63.
7. Wronikowska O, Michalak A, Skalicka-Woźniak K, Crawford AD, Budzyńska B. Fishing for a deeper understanding of nicotine effects using zebrafish behavioural models. Progress in Neuro-Psychopharmacology and Biological Psychiatry. 2020;98:109826.
8. Hoyt ATM, Canfield MAPD, Romitti PAPD, Botto LDMD, Anderka MTSD, Krikov SVM, et al. Associations between Maternal Periconceptional Exposure to Secondhand Tobacco Smoke and Major Birth Defects. American journal of obstetrics and gynecology. 2016;215(5):613.e1-.e11.
9. Budden KF, Shukla SD, Rehman SF, Bowerman KL, Keely S, Hugenholtz P, et al. Functional effects of the microbiota in chronic respiratory disease. Lancet Respir Med. 2019;7(10):907-20.
10. Fricker M, Goggins BJ, Mateer S, Jones B, Kim RY, Gellatly SL, et al. Chronic cigarette smoke exposure induces systemic hypoxia that drives intestinal dysfunction. JCI Insight. 2018;3(3).
11. Bowerman KL, Rehman SF, Vaughan A, Lachner N, Budden KF, Kim RY, et al. Disease-associated gut microbiome and metabolome changes in patients with chronic obstructive pulmonary disease. Nat Commun. 2020;11(1):5886.
12. Malyla V, Paudel KR, Shukla SD, Donovan C, Wadhwa R, Pickles S, et al. Recent advances in experimental animal models of lung cancer. Future Med Chem. 2020;12(7):567-70.
13. Shanahan ER, Shah A, Koloski N, Walker MM, Talley NJ, Morrison M, et al. Influence of cigarette smoking on the human duodenal mucosa-associated microbiota. Microbiome. 2018;6(1):150.
14. Pavia CS, Pierre A, Nowakowski J. Journal of medical microbiology. 2000;49(7):675-6.
15. Jang YO, Kim OH, Kim SJ, Lee SH, Yun S, Lim SE, et al. High-fiber diets attenuate emphysema development via modulation of gut microbiota and metabolism. Scientific reports. 2021;11(1):7008.
16. Jang YO, Lee SH, Choi JJ, Kim DH, Choi JM, Kang MJ, et al. Fecal microbial transplantation and a high fiber diet attenuates emphysema development by suppressing inflammation and apoptosis. Exp Mol Med. 2020;52(7):1128-39.
17. Gosens R, Hiemstra PS, Adcock IM, Bracke KR, Dickson RP, Hansbro PM, et al. Host-microbe cross-talk in the lung microenvironment: implications for understanding and treating chronic lung disease. Eur Respir J. 2020;56(2).
18. Ellis LD, Soo EC, Achenbach JC, Morash MG, Soanes KH. Use of the zebrafish larvae as a model to study cigarette smoke condensate toxicity. PLoS ONE. 2014;9(12):e115305.
19. Alvarez M, Chávez MN, Miranda M, Aedo G, Allende ML, Egaña JT. A Novel In Vivo Model to Study Impaired Tissue Regeneration Mediated by Cigarette Smoke. Scientific reports. 2018;8(1):10926.
20. Palpant NJ, Hofsteen P, Pabon L, Reinecke H, Murry CE. Cardiac Development in Zebrafish and Human Embryonic Stem Cells Is Inhibited by Exposure to Tobacco Cigarettes and E-Cigarettes. PLoS ONE. 2015;10(5):e0126259.

21. Progatzky F, Cook H, Lamb J, Bugeon L, Dallman M. Mucosal inflammation at the respiratory interface: A zebrafish model. American journal of physiology Lung cellular and molecular physiology. 2015;310:ajplung.00323.2015.
22. Massarsky A, Prasad GL, Di Giulio RT. Total particulate matter from cigarette smoke disrupts vascular development in zebrafish brain (Danio rerio). Toxicology and applied pharmacology. 2018;339:85-96.
23. Massarsky A, Jayasundara N, Glazer L, Levin ED, Prasad GL, Di Giulio RT. Outcomes of developmental exposure to total particulate matter from cigarette smoke in zebrafish (Danio rerio). Neurotoxicology. 2018;68:101-14.
24. Renshaw SA, Trede NS. A model 450 million years in the making: zebrafish and vertebrate immunity. Disease models & mechanisms. 2012;5(1):38-47.
25. Hall C, Flores MV, Storm T, Crosier K, Crosier P. The zebrafish lysozyme C promoter drives myeloid-specific expression in transgenic fish. BMC Dev Biol. 2007;7(1):42.
26. Walton EM, Cronan MR, Beerman RW, Tobin DM. The Macrophage-Specific Promoter mfap4 Allows Live, Long-Term Analysis of Macrophage Behavior during Mycobacterial Infection in Zebrafish. PLoS ONE. 2015;10(10):e0138949.
27. Cholan PM, Han A, Woodie BR, Watchon M, Kurz AR, Laird AS, et al. Conserved anti-inflammatory effects and sensing of butyrate in zebrafish. Gut Microbes. 2020;12(1):1-11.
28. Melancon E, Gomez De La Torre Canny S, Sichel S, Kelly M, Wiles TJ, Rawls JF, et al. Best practices for germ-free derivation and gnotobiotic zebrafish husbandry. Methods in cell biology. 2017;138:61-100.
29. Beckett EL, Stevens RL, Jarnicki AG, Kim RY, Hanish I, Hansbro NG, et al. A new short-term mouse model of chronic obstructive pulmonary disease identifies a role for mast cell tryptase in pathogenesis. J Allergy Clin Immunol. 2013;131(3):752-62.
30. Petzold AM, Balciunas D, Sivasubbu S, Clark KJ, Bedell VM, Westcot SE, et al. Nicotine response genetics in the zebrafish. Proc Natl Acad Sci U S A. 2009;106(44):18662-7.
31. Oehlers SH, Flores MV, Okuda KS, Hall CJ, Crosier KE, Crosier PS. A chemical enterocolitis model in zebrafish larvae that is dependent on microbiota and responsive to pharmacological agents. Dev Dyn. 2011;240(1):288-98.
32. Oehlers SH, Flores MV, Hall CJ, Crosier KE, Crosier PS. Retinoic acid suppresses intestinal mucus production and exacerbates experimental enterocolitis. Dis Model Mech. 2012;5(4):457-67.
33. Rawls JF, Mahowald MA, Ley RE, Gordon JI. Reciprocal gut microbiota transplants from zebrafish and mice to germ-free recipients reveal host habitat selection. Cell. 2006;127(2):423-33.
34. Cholan PM, Morris S, Luo K, Chen J, Boland JA, McCaughan GW, et al. Transplantation of high fat fed mouse microbiota into zebrafish embryos identifies pathobiont species. bioRxiv. 2021:2021.04.28.441900.
35. Rutting S, Xenaki D, Malouf M, Horvat JC, Wood LG, Hansbro PM, et al. Short-chain fatty acids increase TNFalpha-induced inflammation in primary human lung mesenchymal cells through the activation of p38 MAPK. American journal of physiology Lung cellular and molecular physiology. 2019;316(1):L157-L74.
36. Oehlers SH, Flores MV, Hall CJ, Wang L, Ko DC, Crosier KE, et al. A whole animal chemical screen approach to identify modifiers of intestinal neutrophilic inflammation. FEBS J. 2017;284(3):402-13.

400 **FIGURE LEGENDS**

401 **Figure 1: Cigarette smoke extract is toxic to zebrafish larvae, and causes increased embryo motility, and**
402 **greater macrophage influx into wounds**

403 A. Survival of 3 dpf larvae after exposure to CSE. Individual Log-rank comparison scores: P(0% vs 1%) =
404 0.3173, P(0% vs 2%) = 0.0798, P(0% vs 3%) <0.0001, P(1 vs 3) <0.0001, P(2% vs 3%) <0.0001. Starting n per
405 group: 0 = 45 larvae, 1% = 45 larvae, 2% = 45 larvae, 3% = 36 larvae.
406 B. Representative images of 5 dpf larvae exposed to CSE from 3 dpf. Scale bar = 1 mm.
407 C. Total distance moved in 15 minutes by 5 dpf larvae exposed to CSE from 3 dpf. Statistical comparison by
408 ANOVA, data are representative of two biological replicates.
409 D. Quantification of neutrophil fluorescent pixel area within 100 µm of the wound margin at 6 hpw in 5 dpf
410 larvae exposed to CSE from 3 dpf. Statistical comparison by ANOVA, data are normalised and combined
411 from two biological replicates.
412 E. Quantification of macrophage fluorescent pixel area within 100 µm of the wound margin at 6 hpw in 5
413 dpf larvae exposed to CSE at doses indicated from 3 dpf. Statistical comparison by ANOVA, data are
414 normalised and combined from two biological replicates.
415

416 **Figure 2: Acute exposure to CSE induces myelopoiesis in zebrafish larvae**

417 A. Representative images of 6 dpf *Tg(lyzC:DsRed)*^{nz50} larvae exposed to CSE for 24 hours from 5 dpf.
418 B. Quantification of total neutrophil fluorescent pixel area in 6 dpf larva exposed to CSE for 24 hours from 5
419 dpf.
420 C. Representative images of 6 dpf *Tg(mfap4:turquoise)*^{xt27} larvae exposed to CSE for 24 hours from 5 dpf.
421 D. Quantification of total macrophage fluorescent pixel area in 6 dpf larva exposed to CSE for 24 hours from
422 5 dpf.
423 A & C: Scale bars = 1 mm. Bounded area in insets are used to measure gut leukocytes in Figure 3 onwards.
424 B & D: Statistical comparison by ANOVA, data are representative of two biological replicates.
425

426 **Figure 3 Acute exposure to CSE induces an inflammatory response in the gut of zebrafish larvae**

427 A. Quantification of gut neutrophil fluorescent pixel area in 6 dpf larvae treated with broad spectrum
428 antibiotics (Abx) ampicillin and kanamycin and exposed to CSE from 5 dpf.
429 B. Quantification of gut macrophage fluorescent pixel area in 6 dpf larvae treated with broad spectrum
430 antibiotics (Abx) ampicillin and kanamycin and exposed to CSE from 5 dpf.
431 Statistical comparisons by ANOVA, data are representative of two biological replicates.
432

433 **Figure 4 CS-exposed mouse microbiota increases the neutrophilic inflammatory effects of CSE**

434 A. Representative images of 5 dpf microbiota-depleted *Tg(lyzC:DsRed)*^{nz50} larvae exposed to combinations
435 of CS- or control normal air-exposed mouse microbiota with or without 1% CSE from 3 dpf.
436 B. Quantification of total neutrophil fluorescent pixel area per larva exposed to combinations of CS- or
437 control normal air-exposed mouse microbiota with or without 1% CSE from 3 dpf. Statistical comparison by
438 ANOVA, data are representative of two biological replicates.
439 C. Representative images of the posterior guts of microbiome depleted *Tg(lyzC:DsRed)*^{nz50} larvae exposed to
440 combinations of CS- or control normal air-exposed mouse microbiota with or without 1% CSE from 3 dpf.
441 Area used for analysis demarcated by yellow box.
442 D. Quantification of gut neutrophil fluorescent pixel area per larva exposed to combinations of CS- or
443 control normal air-exposed mouse microbiota with or without 1% CSE from 3 dpf. Statistical comparison by
444 ANOVA, data are representative of two biological replicates.
445 E. Quantification of *il1b* transcripts by qPCR in larvae exposed to combinations of CS- or control normal air-
446 exposed mouse microbiota with or without 1% CSE from 3 dpf. Statistical comparison by ANOVA, each data
447 point represents a biological replicate with at least 10 larvae per group.
448 Scale bars = 1 mm.
449

450 **Figure 5 CS-exposed mouse microbiota increases the macrophage inflammatory effects of CSE**

451 A. Representative images of 5 dpf microbiota-depleted *Tg(mfap4:turquoise)*^{xt27} larvae exposed to
452 combinations of CS- or control normal air-exposed mouse microbiota with or without 1% CSE from 3 dpf.

453 B. Quantification of total macrophage fluorescent pixel area per larva exposed to combinations of CS- or
454 control normal air-exposed mouse microbiota with or without 1% CSE. Statistical comparison by ANOVA,
455 data are representative of two biological replicates.
456 C. Representative images of the posterior guts of microbiome depleted *Tg(mfap4:turquoise)*^{xt27} larvae
457 exposed to combinations of CS- or control normal air-exposed mouse microbiota with or without 1% CSE.
458 Area used for analysis demarcated by yellow box.
459 D. Quantification of gut macrophage fluorescent pixel area per larva exposed to combinations of CS- or
460 control normal air-exposed mouse microbiota with or without 1% CSE. Statistical comparison by ANOVA,
461 data are representative of two biological replicates.
462 Scale bars indicate 1 mm.
463
464 **Figure 6 CS-exposed faecal microbiota contain culturable bacteria that do not affect inflammatory**
465 **responses**
466 A. Quantification of total neutrophil fluorescent pixel area per larva exposed to bacterial isolates with or
467 without 1% CSE.
468 B. Quantification of gut neutrophil fluorescent pixel area per larva exposed to bacterial isolates with or
469 without 1% CSE.
470 C. Quantification of total macrophage fluorescent pixel area per larva exposed to bacterial isolates with or
471 without 1% CSE.
472 D. Quantification of gut macrophage fluorescent pixel area per larva exposed to bacterial isolates with or
473 without 1% CSE. Statistical comparisons by ANOVA.
474

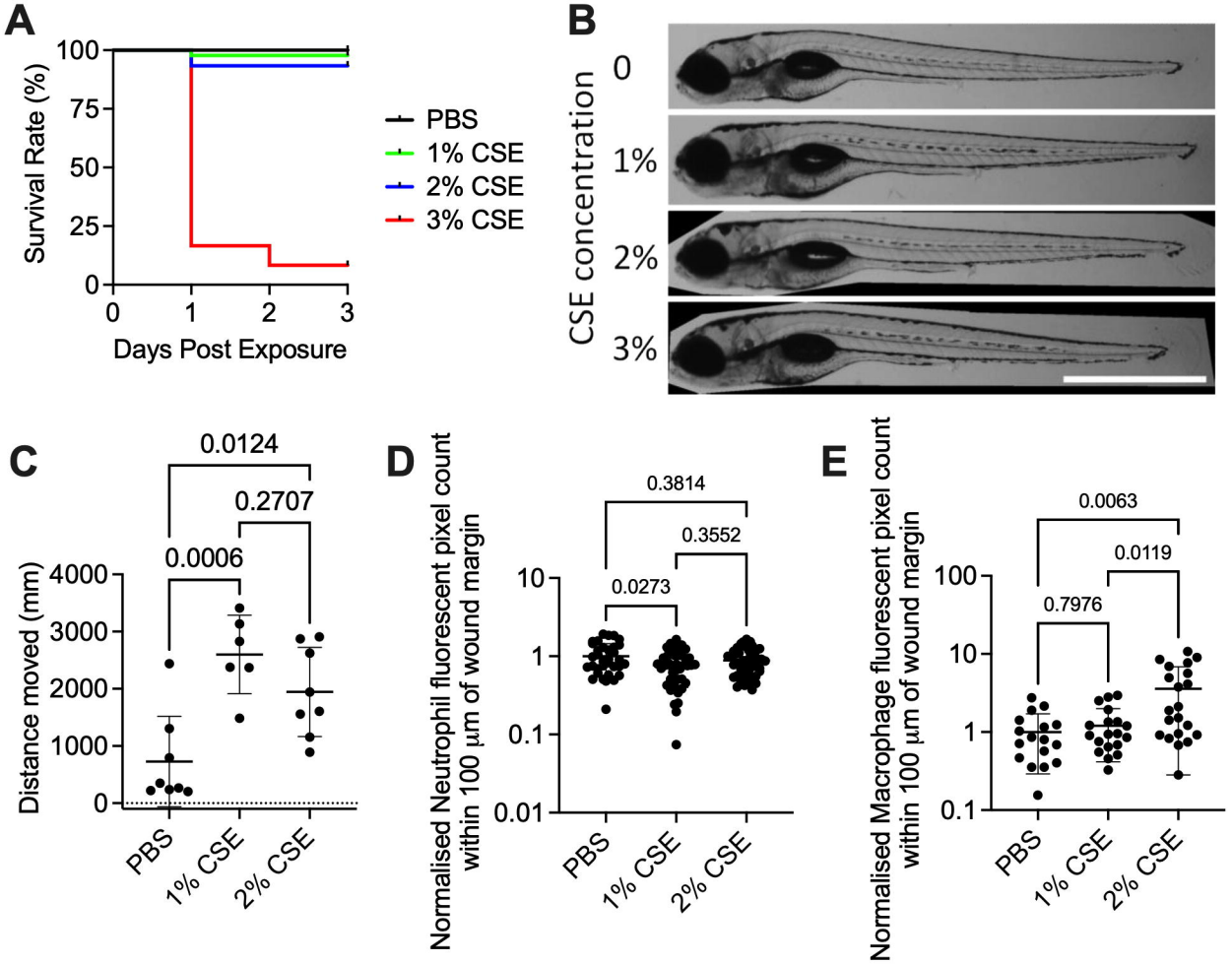
A
Survival Rate (%)
100
75
50
25
0
0
1
2
3
Days Post Exposure
PBS
1% CSE
2% CSE
3% CSE
B
CSE concentration
0
1%
2%
3%
C
0.0124
0.2707
0.0006
Distance moved (mm)
4000
3000
2000
1000
0
PBS
1% CSE
2% CSE
D
0.3814
0.3552
0.0273
Normalised Neutrophil fluorescent pixel count within 100 μm of wound margin
10
1
0.1
0.01
PBS
1% CSE
2% CSE
E
0.0063
0.0119
0.7976
Normalised Macrophage fluorescent pixel count within 100 μm of wound margin
100
10
1
0.1
PBS
1% CSE
2% CSE

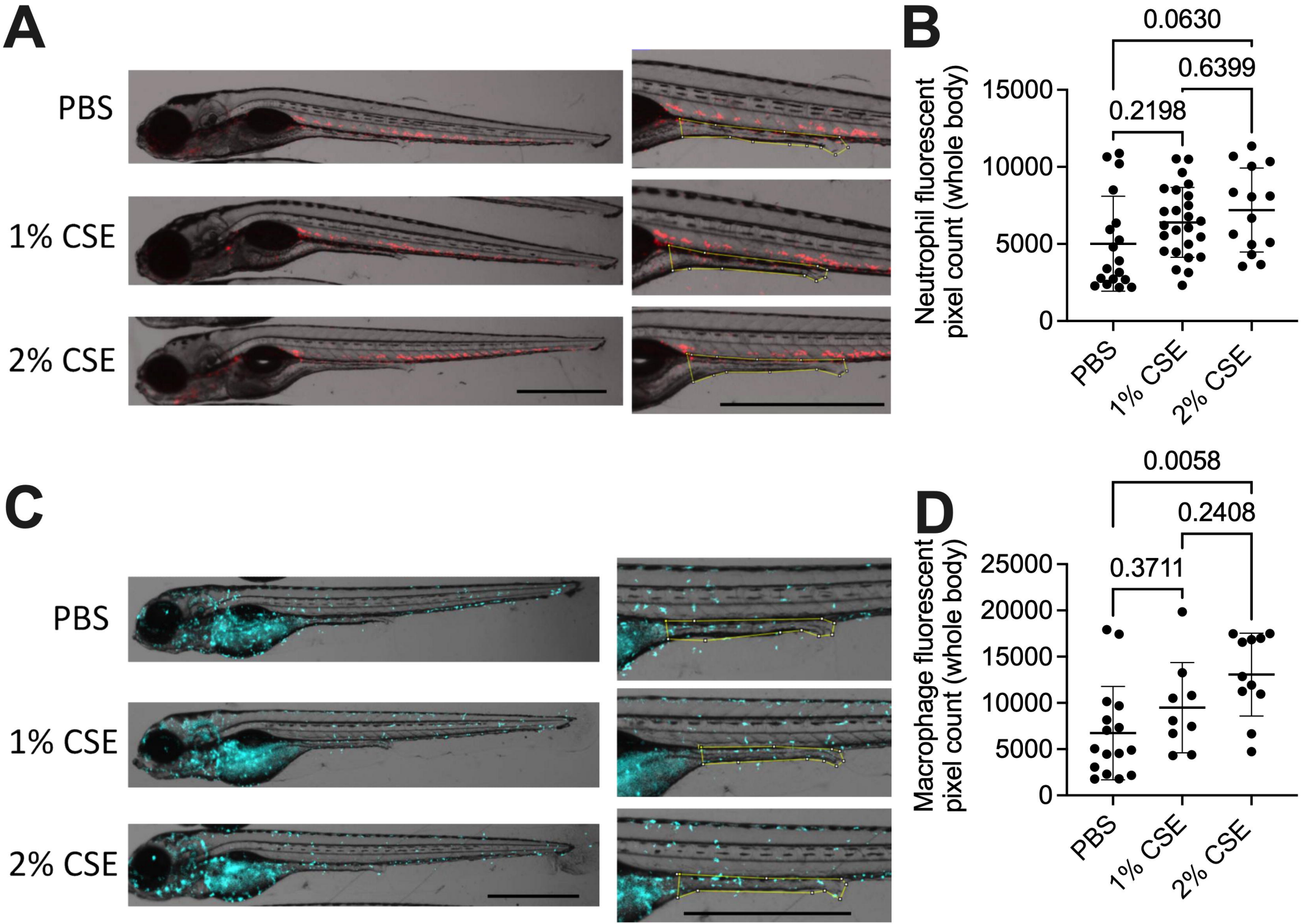
A
PBS
1% CSE
2% CSE
B
0.0630
0.6399
0.2198
Neutrophil fluorescent pixel count (whole body)
15000
10000
5000
0
PBS
1% CSE
2% CSE
C
PBS
1% CSE
2% CSE
D
0.0058
0.2408
0.3711
Macrophage fluorescent pixel count (whole body)
25000
20000
15000
10000
5000
0
PBS
1% CSE
2% CSE

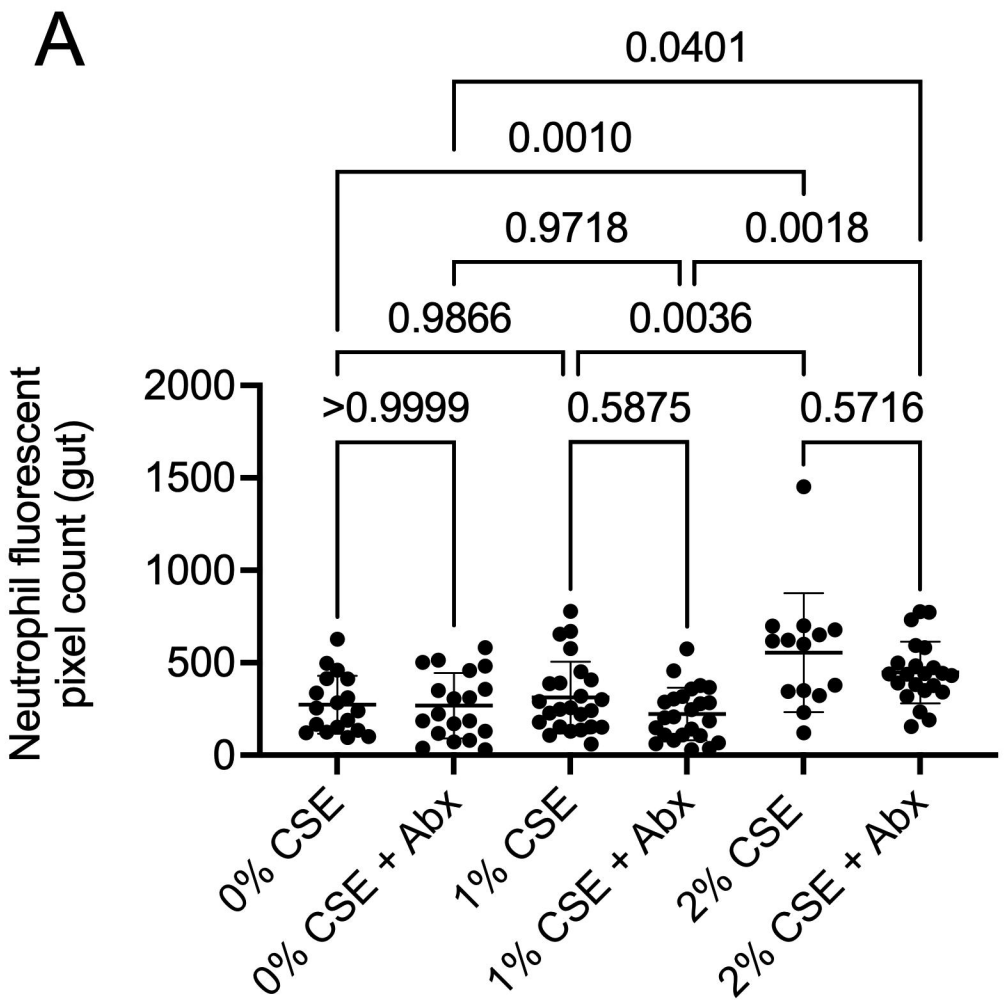
A
0.0401
0.0010
0.9718
0.0018
0.9866
0.0036
>0.9999
0.5875
0.5716
Neutrophil fluorescent pixel count (gut)
2000
1500
1000
500
0
0% CSE
0% CSE + Abx
1% CSE
1% CSE + Abx
2% CSE
2% CSE + Abx

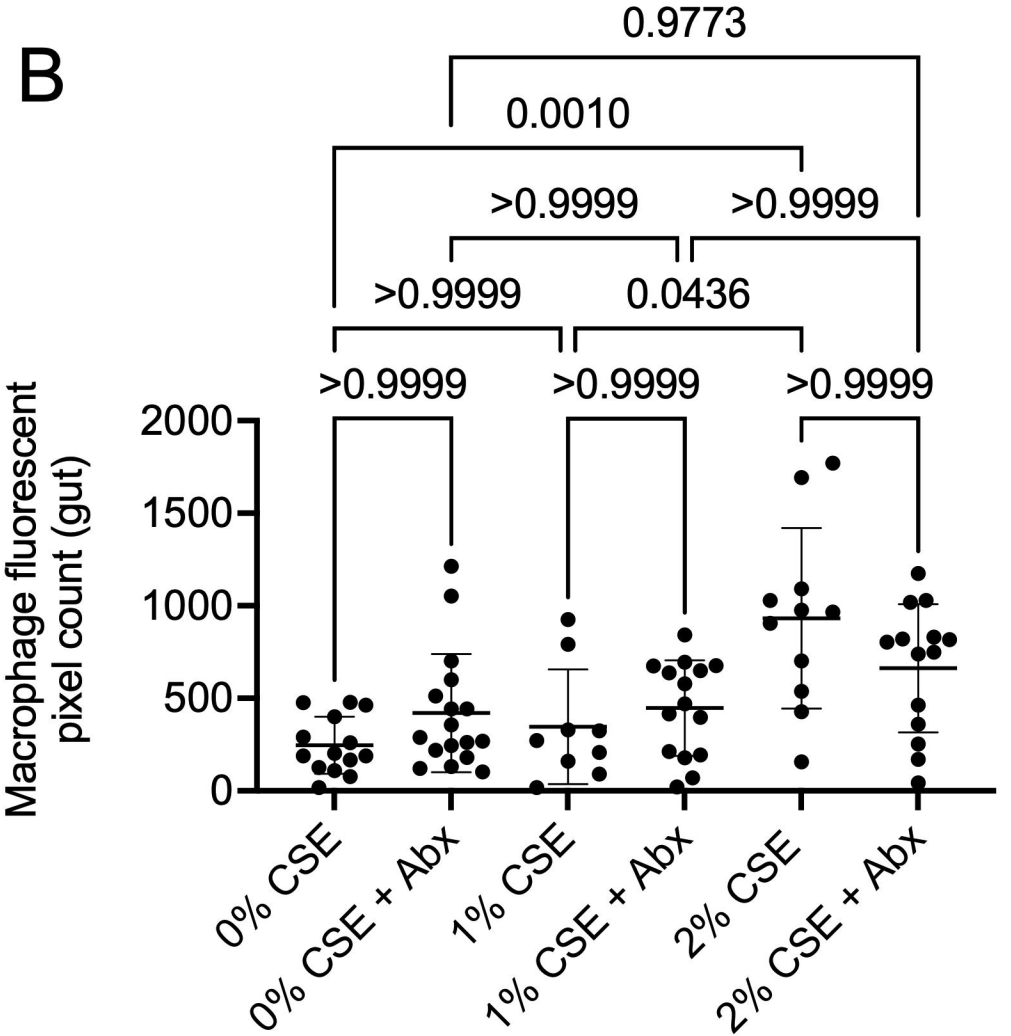
B
0.9773
0.0010
>0.9999
>0.9999
>0.9999
0.0436
>0.9999
>0.9999
>0.9999
Macrophage fluorescent pixel count (gut)
2000
1500
1000
500
0
0% CSE
0% CSE + Abx
1% CSE
1% CSE + Abx
2% CSE
2% CSE + Abx

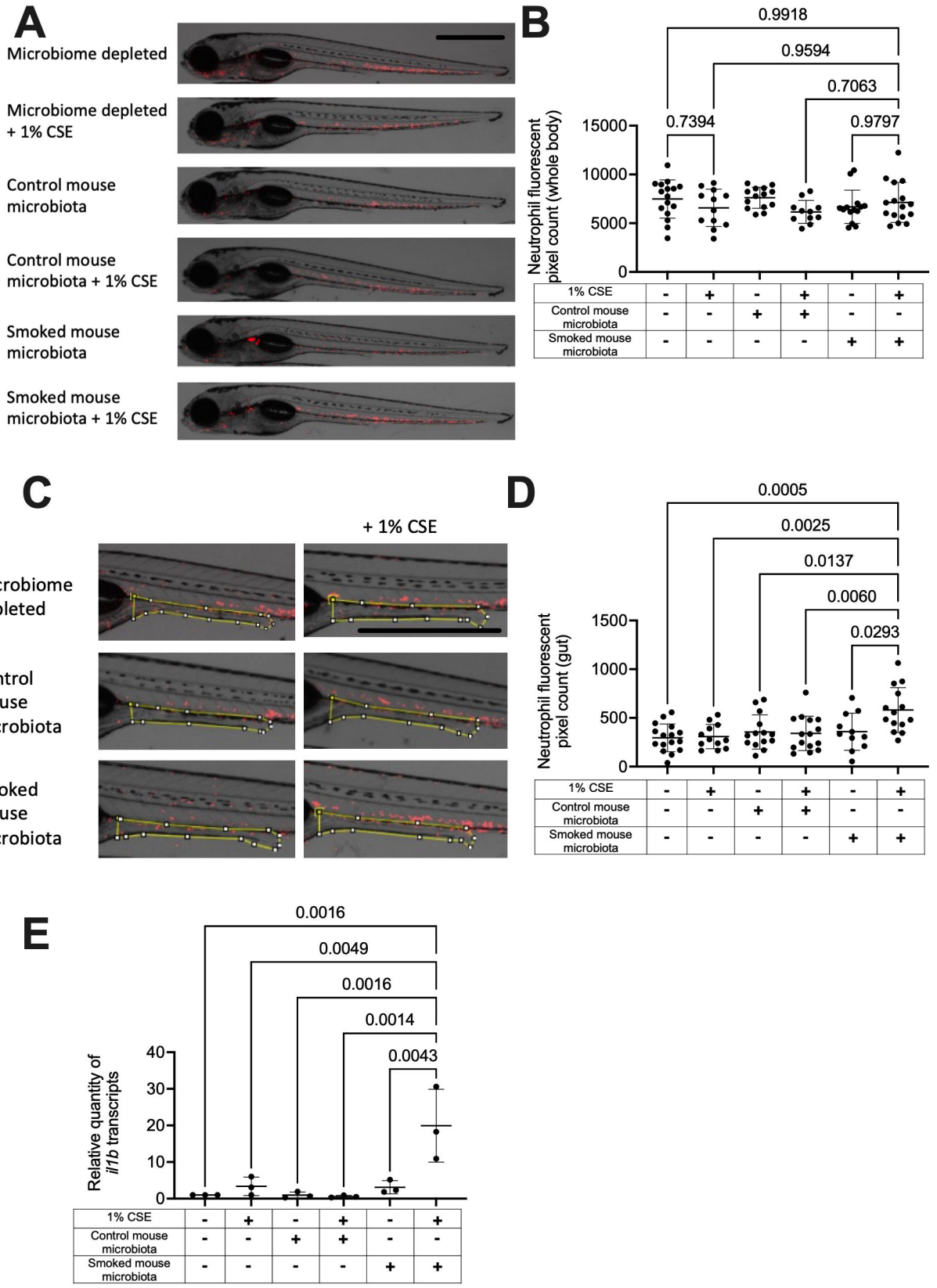
A
Microbiome depleted
Microbiome depleted + 1% CSE
Control mouse microbiota
Control mouse microbiota + 1% CSE
Smoked mouse microbiota
Smoked mouse microbiota + 1% CSE
B
0.9918
0.9594
0.7063
0.7394
0.9797
Neutrophil fluorescent pixel count (whole body)
15000
10000
5000
0
1% CSE
Control mouse microbiota
Smoked mouse microbiota
C
+ 1% CSE
Microbiome depleted
Control mouse microbiota
Smoked mouse microbiota
D
0.0005
0.0025
0.0137
0.0060
0.0293
Neutrophil fluorescent pixel count (gut)
1500
1000
500
0
1% CSE
Control mouse microbiota
Smoked mouse microbiota
E
0.0016
0.0049
0.0016
0.0014
0.0043
Relative quantity of il1b transcripts
40
30
20
10
0
1% CSE
Control mouse microbiota
Smoked mouse microbiota

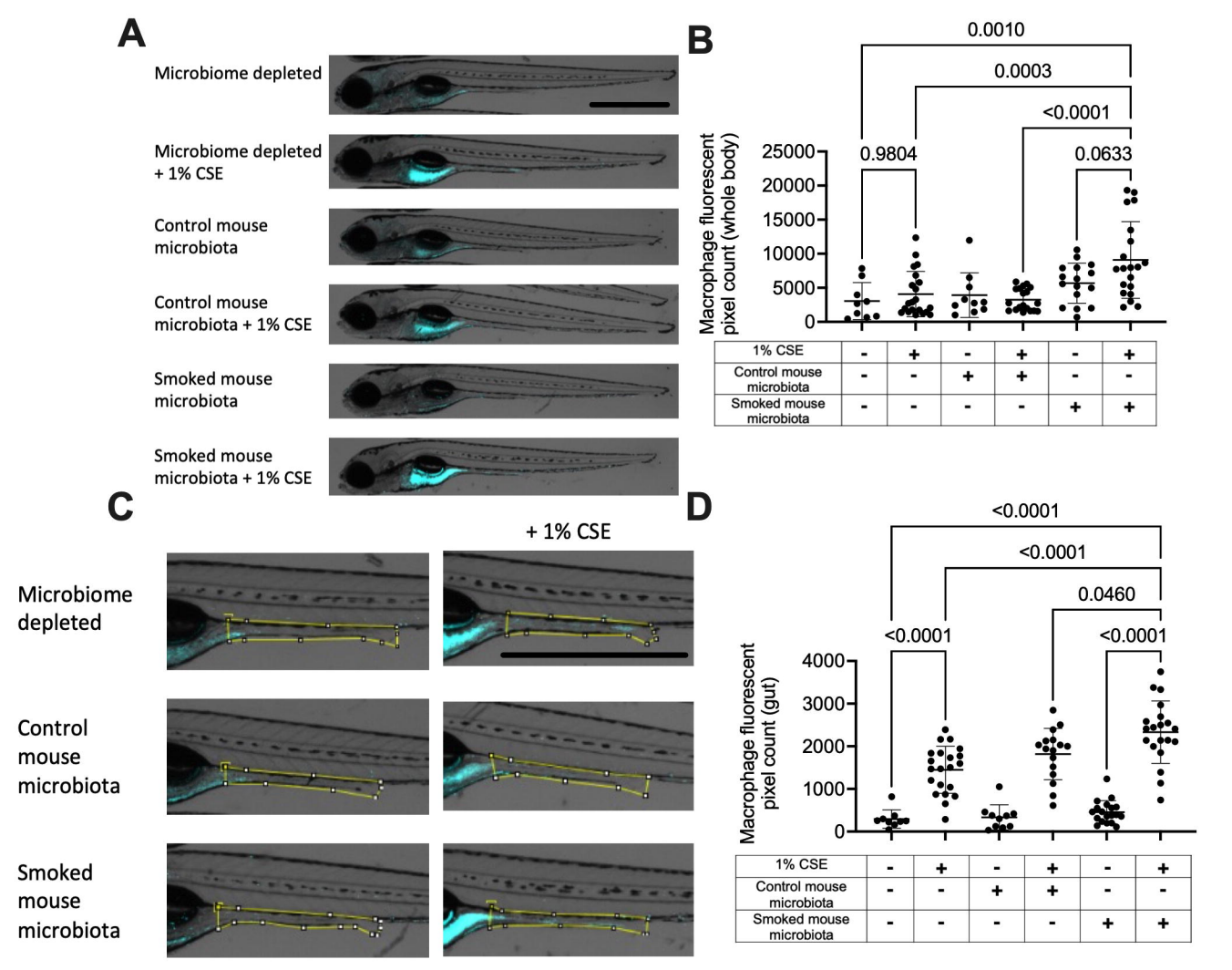
A
Microbiome depleted
Microbiome depleted + 1% CSE
Control mouse microbiota
Control mouse microbiota + 1% CSE
Smoked mouse microbiota
Smoked mouse microbiota + 1% CSE
B
Macrophage fluorescent pixel count (whole body)
25000
20000
15000
10000
5000
0
0.0010
0.0003
<0.0001
0.9804
0.0633
1% CSE
Control mouse microbiota
Smoked mouse microbiota
C
+ 1% CSE
Microbiome depleted
Control mouse microbiota
Smoked mouse microbiota
D
Macrophage fluorescent pixel count (gut)
4000
3000
2000
1000
0
<0.0001
<0.0001
0.0460
<0.0001
<0.0001
1% CSE
Control mouse microbiota
Smoked mouse microbiota

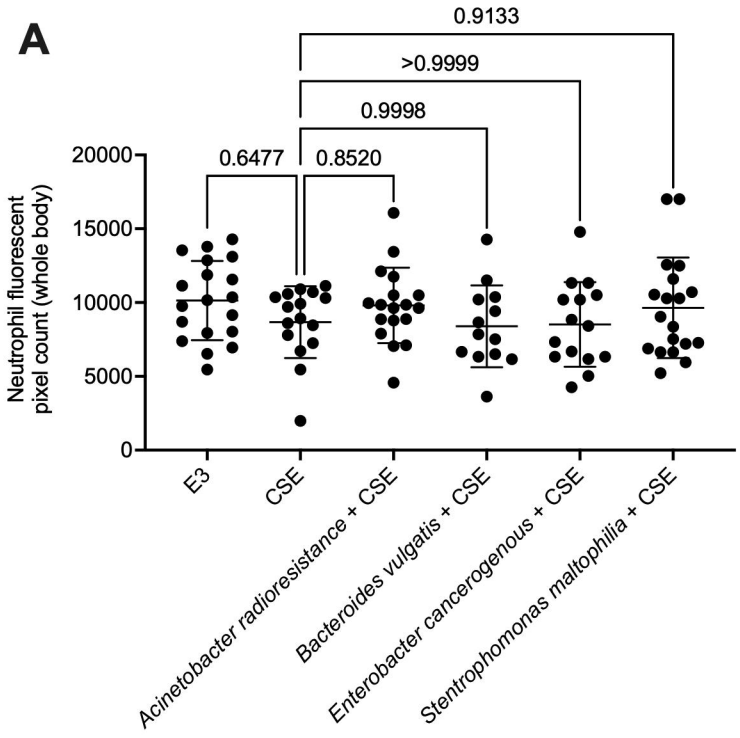
A
0.9133
>0.9999
0.9998
0.6477
0.8520
20000
15000
10000
5000
0
Neutrophil fluorescent pixel count (whole body)
E3
CSE
Acinetobacter radioresistance + CSE
Bacteroides vulgatis + CSE
Enterobacter cancerogenous + CSE
Stentrophomonas maltophilia + CSE

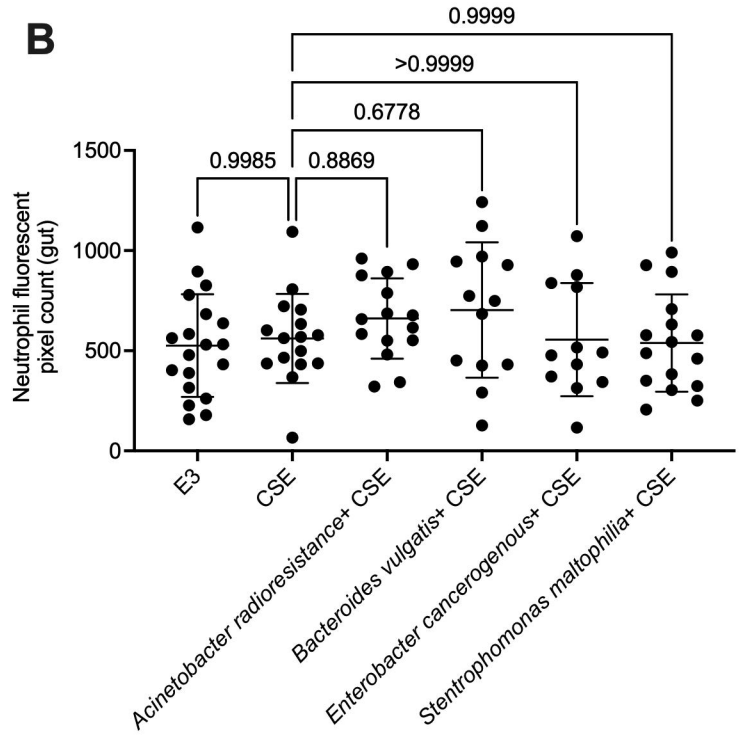
B
0.9999
>0.9999
0.6778
0.9985
0.8869
1500
1000
500
0
Neutrophil fluorescent pixel count (gut)
E3
CSE
Acinetobacter radioresistance+ CSE
Bacteroides vulgatis+ CSE
Enterobacter cancerogenous+ CSE
Stentrophomonas maltophilia+ CSE

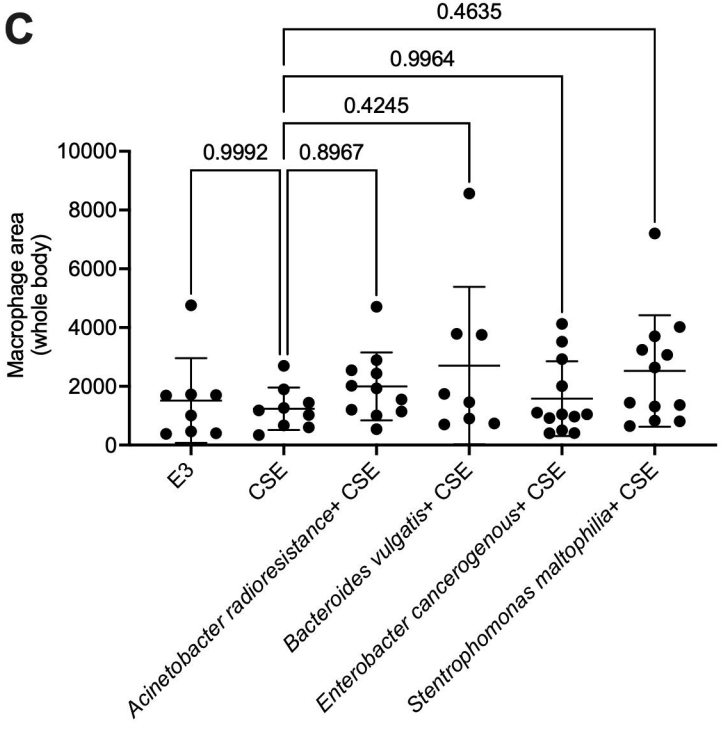
C
0.4635
0.9964
0.4245
0.9992
0.8967
10000
8000
6000
4000
2000
0
Macrophage area (whole body)
E3
CSE
Acinetobacter radioresistance+ CSE
Bacteroides vulgatis+ CSE
Enterobacter cancerogenous+ CSE
Stentrophomonas maltophilia+ CSE

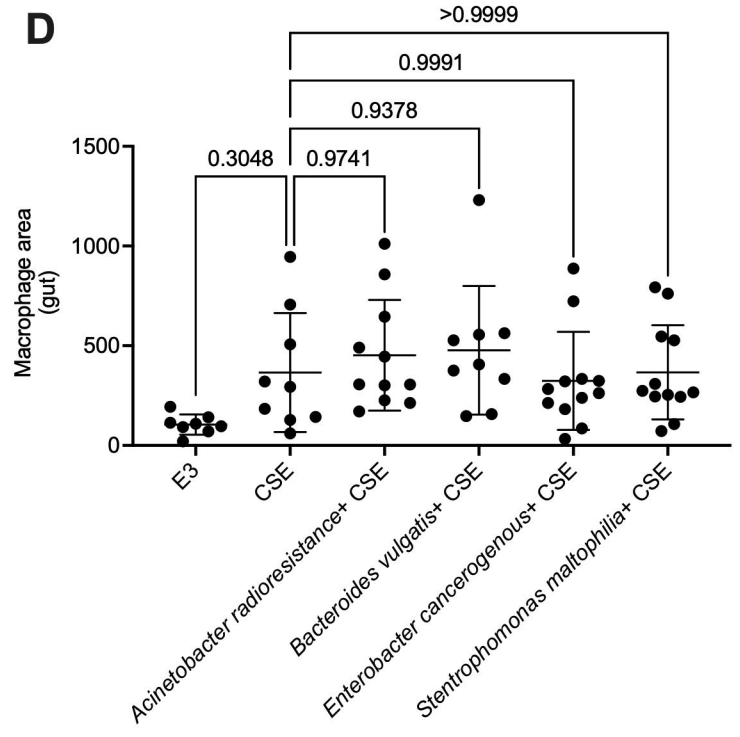
D
>0.9999
0.9991
0.9378
0.3048
0.9741
1500
1000
500
0
Macrophage area (gut)
E3
CSE
Acinetobacter radioresistance+ CSE
Bacteroides vulgatis+ CSE
Enterobacter cancerogenous+ CSE
Stentrophomonas maltophilia+ CSE